

## Supplementary Information for article

### *Exceptional structural diversity of hybrid halocuprates(I) with methylammonium and formamidinium cations*

Daria E. Belikova<sup>a</sup>, Sergey A. Fateev<sup>a</sup>, Victor N. Khrustalev<sup>bc</sup>, Ekaterina I. Marchenko<sup>ad</sup>, Eugene A. Goodilin<sup>ae</sup>, Shenghao Wang<sup>f\*</sup>, Alexey B. Tarasov<sup>ae\*</sup>

<sup>a</sup> Laboratory of New Materials for Solar Energetics, Faculty of Materials Science, Lomonosov Moscow State University, 119991 Moscow, Russian Federation.

<sup>b</sup> Inorganic Chemistry Department, Peoples' Friendship University of Russia (RUDN University), 117198 Moscow, Russian Federation

<sup>c</sup> Zelinsky Institute of Organic Chemistry, Russian Academy of Sciences, Leninsky Prospekt 47, Moscow 119991, Russia

<sup>d</sup> Department of Geology, M. V. Lomonosov Moscow State University, 119991 Moscow, Russian Federation

<sup>e</sup> Department of Chemistry, Lomonosov Moscow State University, 119991 Moscow, Russian Federation

<sup>f</sup> Materials Genome Institute, Shanghai University, 99 Shangda Road, BaoShan District, Shanghai, 200444, China.

\* Corresponding authors: [shenghaowang@shu.edu.cn](mailto:shenghaowang@shu.edu.cn) and [alexey.bor.tarasov@yandex.ru](mailto:alexey.bor.tarasov@yandex.ru)

Table S1. Parameters of the crystal structure refinement.

Phase	MACu <sub>2</sub> Br <sub>3</sub>	FA <sub>2</sub> Cu <sub>4</sub> Br <sub>6</sub>	MACuBr <sub>2</sub>	FACuBr <sub>2</sub>	FA <sub>3</sub> CuBr <sub>4</sub>	DMFH <sub>2</sub> Cu <sub>3</sub> Br <sub>4</sub>
Empirical formula	CH <sub>6</sub> Br <sub>3</sub> Cu <sub>2</sub> N	CH <sub>5</sub> Br <sub>3</sub> Cu <sub>2</sub> N <sub>2</sub>	CH <sub>6</sub> Br <sub>2</sub> CuN	CH <sub>5</sub> Br <sub>2</sub> CuN <sub>2</sub>	C <sub>3</sub> H <sub>15</sub> Br <sub>4</sub> CuN <sub>6</sub>	C <sub>6</sub> H <sub>15</sub> Br <sub>4</sub> Cu <sub>3</sub> N <sub>2</sub> O <sub>2</sub>
M, g/mol	398.87	411.87	255.42	268.42	518.36	657.45
Crystal system	Monoclinic	Monoclinic	Monoclinic	Monoclinic	Tetragonal	Orthorhombic
Space group	P2 <sub>1</sub> /m	C2/c	C2/m	C 2/m	P <sup>4</sup> 2 <sub>1</sub> m	Pccn
a, Å	8.4716(6)	11.6122(5)	13.6073(8)	12.0193(3)	13.4047(6)	15.7900(9)
b, Å	5.5703(3)	11.5268(4)	5.4260(3)	9.1772(3)	13.4047(6)	15.8919(8)
c, Å	8.4791(9)	12.5098(6)	8.3933(5)	5.8643(2)	8.4141(6)	6.2660(3)
α, deg.	90.000	90.000	90	90.000	90.000	90.000
β, deg.	112.383(10)	110.171(5)	114.5389(15)	114.1620(10)	90.000	90.000
γ, deg.	90.000	90.000	90	90.000	90.000	90.000
V, Å <sup>3</sup>	369.98(6)	1571.76(13)	563.73(6)	590.18(3)	1511.90(17)	1572.35(14)
Z	2	8	4	4	4	4
D (calc), g/cm <sup>3</sup>	3.580	3.481	3.010	3.021	2.227	2.777

$\mu$ , mm <sup>-1</sup>	21.836	20.570	17.891	17.102	11.996	14.176
F(000)	364	1504	472	496	976	1232
Crystal size, mm	0.21×0.12×0.1 1	0.12×0.06×0.0 6	0.24×0.09×0.06	0.30×0.24×0.21	0.21×0.02×0.01	0.21×0.12×0.11
$\Theta$ range for data collection, deg.	2.60 – 29.99	2.57 – 28.00	4.10 – 32.60	2.89 – 32.70	2.15 – 32.62	2.60 – 29.99
Index ranges	-11 ≤ $h$ ≤ 11 -7 ≤ $k$ ≤ 7 -9 ≤ $l$ ≤ 11	-15 ≤ $h$ ≤ 15 -15 ≤ $k$ ≤ 15 -16 ≤ $l$ ≤ 16	-20 ≤ $h$ ≤ 20 -8 ≤ $k$ ≤ 8 -12 ≤ $l$ ≤ 12	-18 ≤ $h$ ≤ 18 -13 ≤ $k$ ≤ 13 -8 ≤ $l$ ≤ 8	-20 ≤ $h$ ≤ 20 -20 ≤ $k$ ≤ 20 -12 ≤ $l$ ≤ 12	-23 ≤ $h$ ≤ 23 -24 ≤ $k$ ≤ 24 -9 ≤ $l$ ≤ 9
Reflections collected/independent	3408/1111	11005/1885	9622/1110	7299/1146	37001/2865	29951/2860
R <sub>int</sub>	0.1073	0.1146	0.0391	0.0509	0.1006	0.0961
Reflections with I > 2σ(I)	975	1654	1078	1106	1735	1705
Goodness-of-fit on F	1.046	1.064	1.033	1.019	1.005	1.001
Final R indices [I > 2σ(I)]	R <sub>1</sub> = 0.0690 wR <sub>2</sub> = 0.1558	R <sub>1</sub> = 0.0573 wR <sub>2</sub> = 0.1460	R <sub>1</sub> = 0.0169 wR <sub>2</sub> = 0.0409	R <sub>1</sub> = 0.0222 wR <sub>2</sub> = 0.0547	R <sub>1</sub> = 0.0970 wR <sub>2</sub> = 0.1862	R <sub>1</sub> = 0.0788 wR <sub>2</sub> = 0.0624
R indices (all data)	R <sub>1</sub> = 0.0731 wR <sub>2</sub> = 0.1590	R <sub>1</sub> = 0.0642 wR <sub>2</sub> = 0.1514	R <sub>1</sub> = 0.0177 wR <sub>2</sub> = 0.0413	R <sub>1</sub> = 0.0233 wR <sub>2</sub> = 0.0551	R <sub>1</sub> = 0.1521 wR <sub>2</sub> = 0.2154	R <sub>1</sub> = 0.0788 wR <sub>2</sub> = 0.0768
T <sub>min</sub> / T <sub>max</sub>	0.007 / 0.077	0.082 / 0.262	0.097 / 0.216	0.006 / 0.018	0.181 / 0.878	0.139/0.765
Largest diff. peak/hole, e/Å <sup>3</sup>	2.248/-2.932	2.540/-1.994	0.625 / -0.706	1.115/-1.770	2.117/-2.241	1.359/-0.903

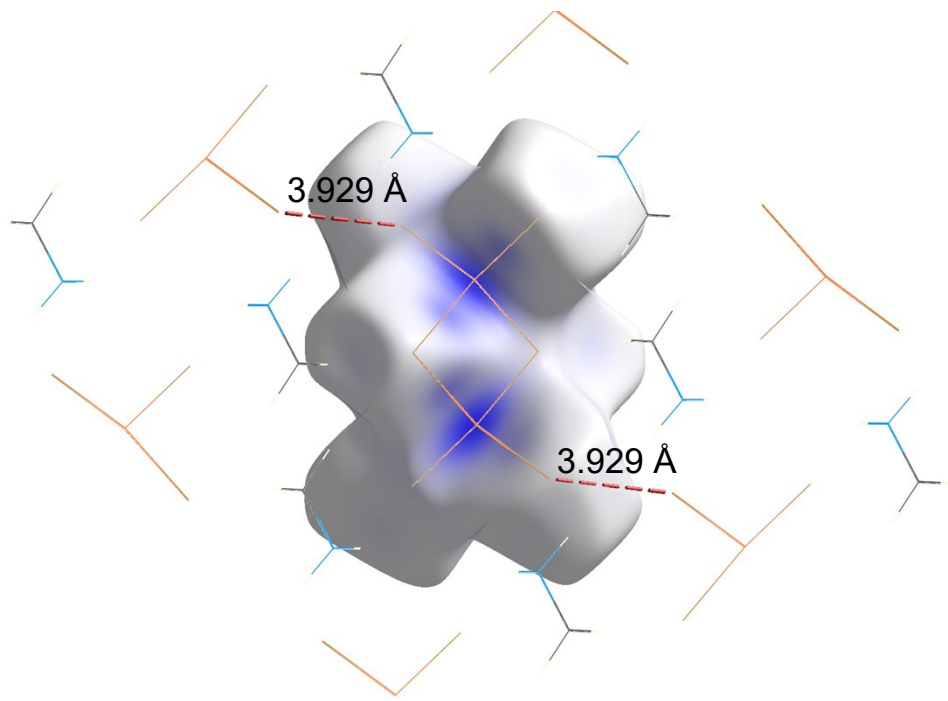


Figure S1. Hirshfeld surface of the  $[\text{Cu}_2\text{Br}_6]^{4-}$  unit of the  $\text{MACu}_2\text{Br}_3$ .

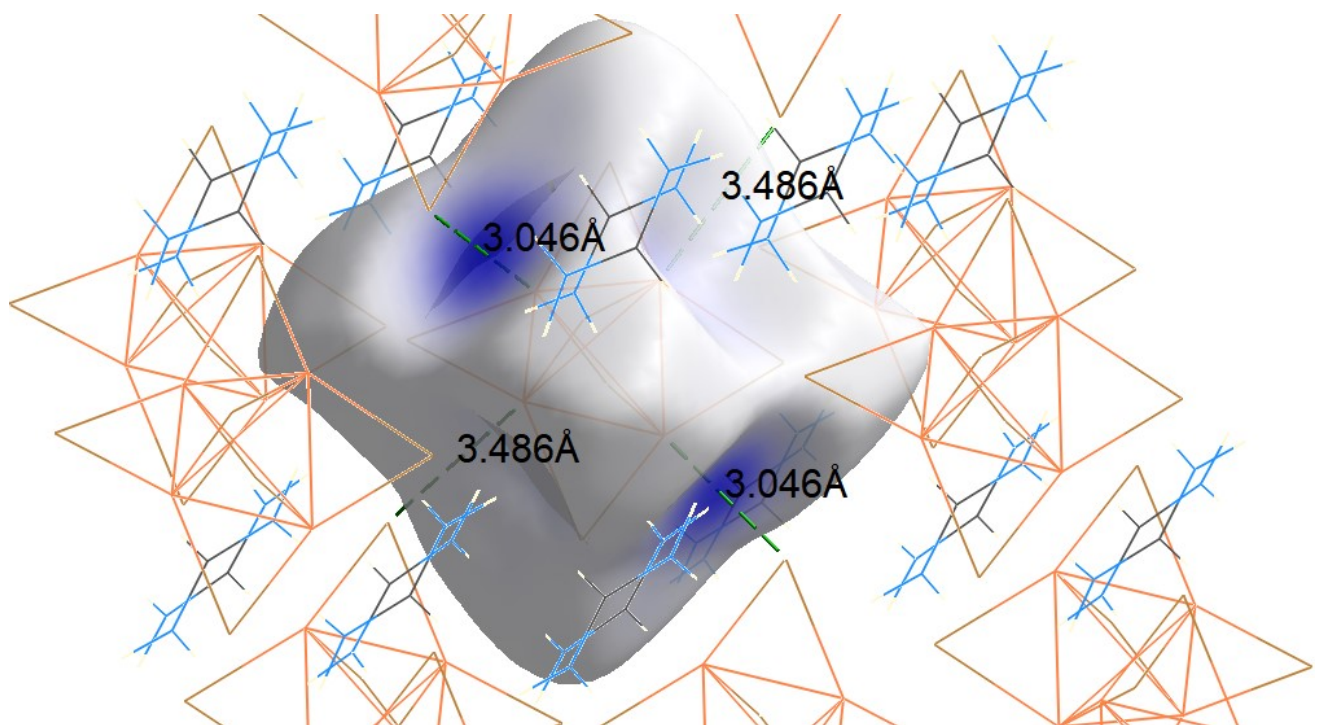


Figure S2. Hirshfeld surface of the  $[\text{Cu}_4\text{Br}_6]^{2-}$  unit of the  $\text{FA}_2[\text{Cu}_4\text{Br}_6]$ .

Table S2. Parameters of the bond lengths and main distances in all studied structures.

Phase	Cu-Br bond length, Å	Distortion index (bond length) <sup>1</sup>	Br-Cu-Br angles, deg.	Bond angle variance <sup>2</sup> , deg. <sup>2</sup>	Shortest Br···Br distance **, Å	Cu···Cu distances, Å	Reference
CsCu <sub>2</sub> Br <sub>3</sub>	2.42658 2.57098 2.57098 2.42658	0.02890	106.4096(0) 108.1509(0) 116.4758(0) 108.1509(0) 108.6056(0) 108.6056(0)	12.6846	3.880	2.90660	<sup>3</sup>
MACu <sub>2</sub> Br <sub>3</sub>	2.4436(14) 2.5648(11) 2.5452(13) 2.4415(12)	0.02251	112.03(4) 109.74(6) 111.23(4) 105.57(6) 101.21(4) 115.99(5)	27.1412	3.929	2.754 2.816	This work
CsCu <sub>2</sub> I <sub>3</sub>	2.60353 2.70349 2.70349 2.60353	0.01883	108.9107(0) 107.0079(0) 114.2395(0) 107.0079(0) 109.7974(0) 109.7974(0)	7.0799	4.1259	3.14327	<sup>3</sup>
MACu <sub>2</sub> I <sub>3</sub>	2.636(4) 2.636(4) 2.710(4) 2.683(4)	0.01136	113.37(10) 103.65(12) 106.62(9) 107.46(13) 111.49(15) 114.07(16)	17.3062	4.248(3)	2.883(9)	<sup>4</sup>
FACu <sub>2</sub> I <sub>3</sub>	2.7126(5) 2.7126(5) 2.6401(5) 2.6401(5)	0.01353	106.29(3) 105.321(10) 114.97(3) 105.321(10) 112.369(7) 112.369(7)	18.3261	4.5712(5)	4.5712(5)	<sup>5</sup>
FA <sub>2</sub> [Cu <sub>4</sub> Br <sub>6</sub> ]*	2.3848(14) 2.3971(12) 2.4011(12)	0.00266	121.28(5) 118.17(5) 120.55(5)	2.6449	3.896	2.8880	This work
MACuBr <sub>2</sub>	2.4898(4) 2.4905(3) 2.4905(3) 2.4898(4)	0.00014	106.139(8) 106.139(8) 108.366(10) 108.366(10) 111.947(13) 116.000(14)	14.6801	4.029	2.639 2.787	This work
FACuBr <sub>2</sub>	2.5177(6) 2.4834(4) 2.4739(4) 2.4739(4)	0.00613	112.246(19) 110.482(10) 110.482(10) 103.201(18) 110.031(10) 110.031(10)	9.9354	4.367	2.758 3.106	This work
FA <sub>3</sub> CuBr <sub>4</sub>	2.506(5) 2.458(3) 2.458(3)	0.00778	116.52(15) 109.88(12) 105.47(14)	16.3814	4.563	8.174	This work

	2.450(4)		105.47(14) 109.61(14) 109.61(14)			
--	----------	--	----------------------------------------	--	--	--

\* Distortion index and bond angle variance are calculated for three-coordinated copper atom.

\*\* Shortest Br···Br distances for all structures are listed for bromine atoms of separate units (i.e. adjacent chains or clusters).

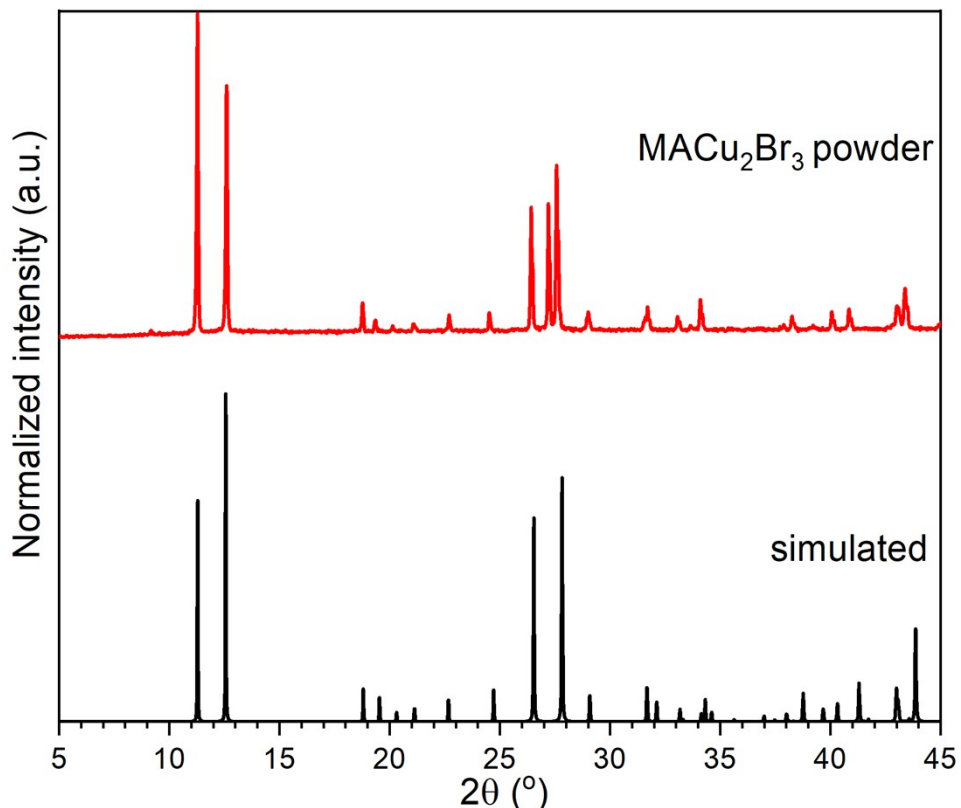


Figure S3. XRD pattern of the synthesized MACu<sub>2</sub>Br<sub>3</sub> powder in comparison with the calculated pattern.

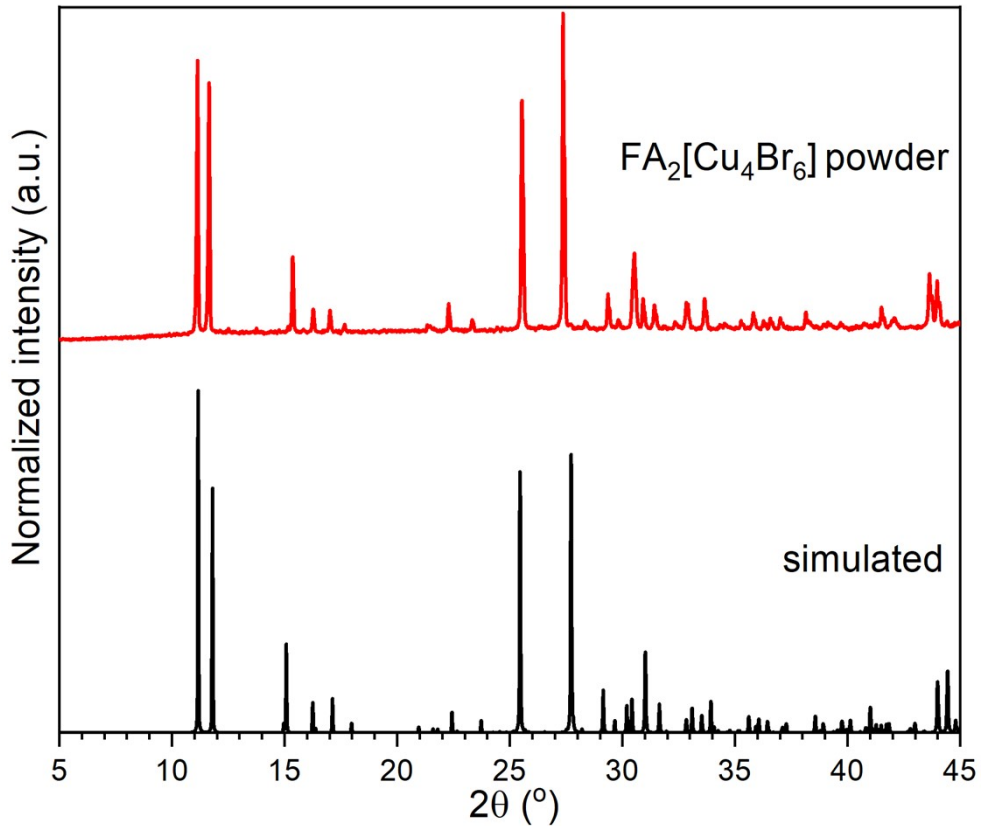


Figure S4. XRD pattern of the synthesized  $\text{FA}_2[\text{Cu}_4\text{Br}_6]$  powder in comparison with the calculated pattern.

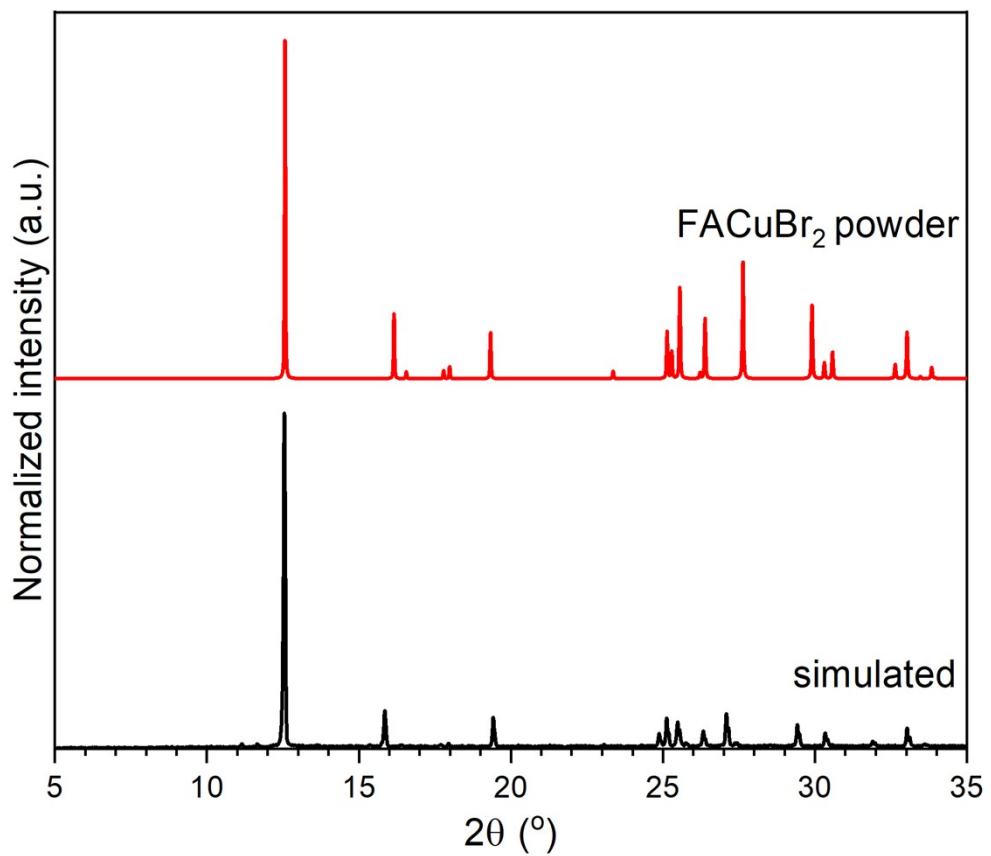


Figure S5. XRD pattern of the synthesized  $\text{FACuBr}_2$  powder in comparison with the calculated pattern.

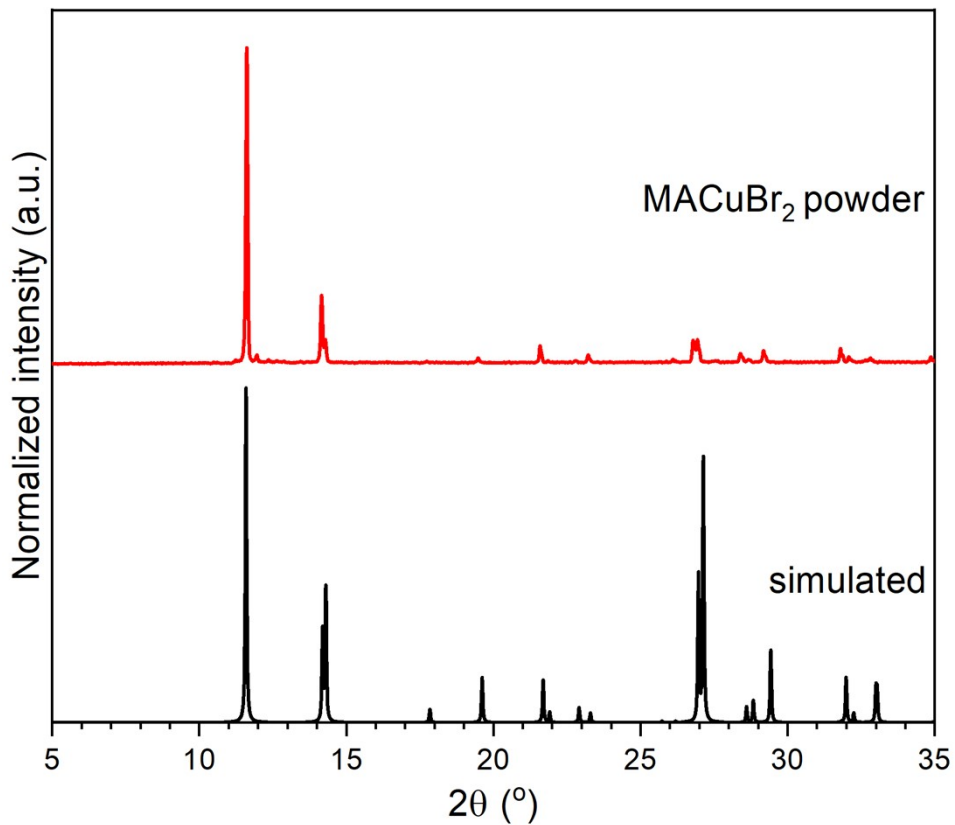


Figure S6. XRD pattern of the synthesized  $\text{MACuBr}_2$  powder in comparison with the calculated pattern.

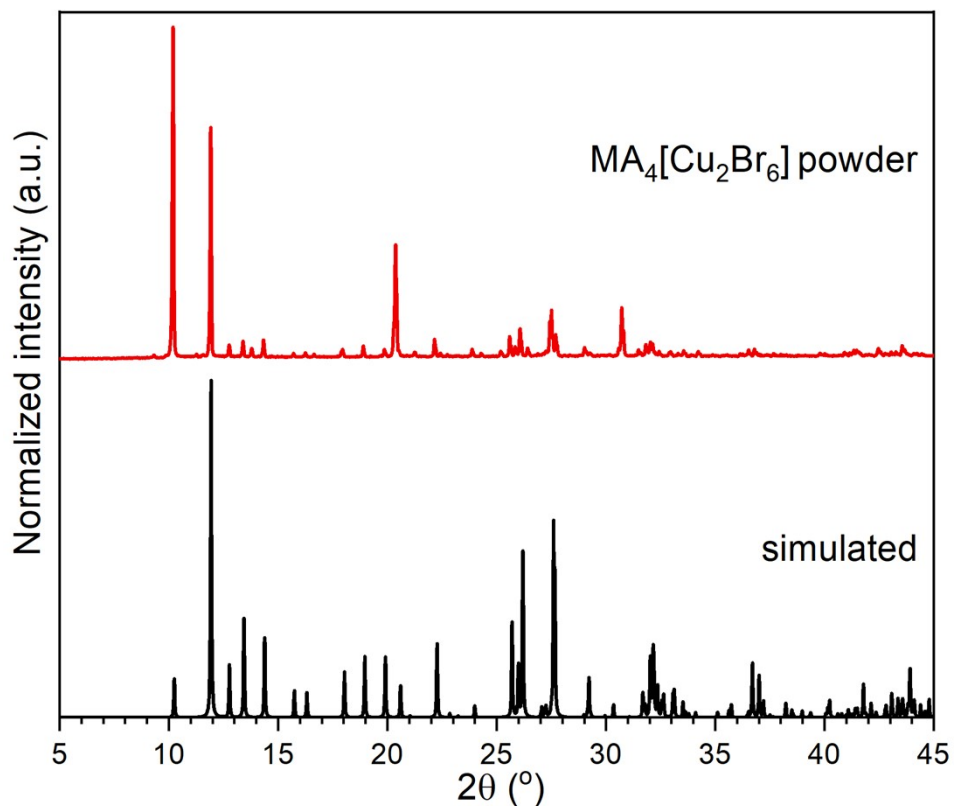


Figure S7. XRD pattern of the synthesized  $\text{MA}_4[\text{Cu}_2\text{Br}_6]$  powder in comparison with the calculated pattern.

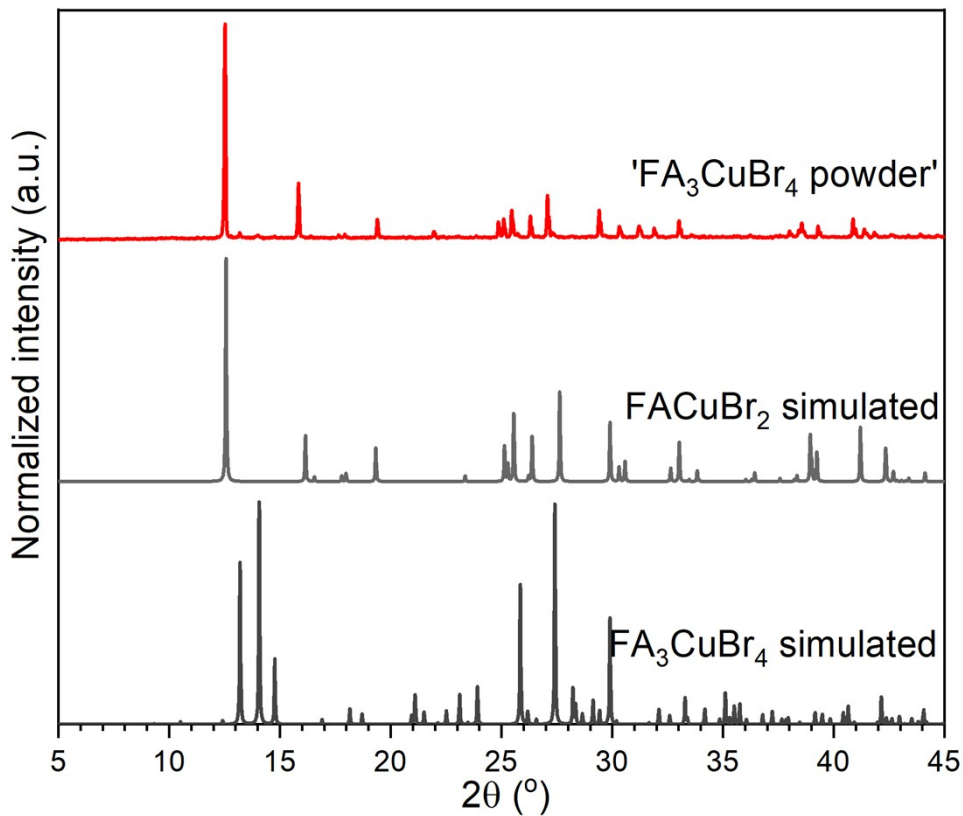


Figure S8. XRD pattern of the synthesized 'FA<sub>3</sub>CuBr<sub>4</sub>' powder in comparison with the calculated patterns of FACuBr<sub>2</sub> and FA<sub>3</sub>CuBr<sub>4</sub>.

Table S3. Optical properties of the studied phases in comparison with other known halocuprates

Phase	PL maximum, eV	Optical bandgap, eV	Stokes Shift, eV	Reference
MACu <sub>2</sub> Br <sub>3</sub>	1.89	3.63	1.74	This work
Cs <sub>2</sub> CuBr <sub>3</sub>	2.23	3.64	1.41	<sup>6</sup>
FA <sub>2</sub> [Cu <sub>4</sub> Br <sub>6</sub> ]	1.99	3.16	1.17	This work
[N(C <sub>4</sub> H <sub>9</sub> ) <sub>3</sub> CH <sub>3</sub> ] <sub>2</sub> [Cu <sub>4</sub> Br <sub>6</sub> ]	1.99	3.01	1.02	<sup>7</sup>
MACuBr <sub>2</sub>	2.30	3.78	1.48	This work
FACuBr <sub>2</sub>	2.53	3.88	1.35	This work
PEACuBr <sub>2</sub> (PEA <sup>+</sup> = phenylethylammonium)	-	3.87	-	<sup>8</sup>
MA <sub>4</sub> [Cu <sub>2</sub> Br <sub>6</sub> ]	2.40	3.91	1.51	This work, <sup>9</sup>
FA <sub>3</sub> CuBr <sub>4</sub>	1.99; 2.52	3.23; 3.89	-	This work

Table S4. Correlations of lattice distortions (A···Cu distances) with PLQY for inorganic and hybrid halocuprates with small organic cations.

Phase	Distortion index (bond length) <sup>1</sup>	Bond angle variance <sup>2</sup> , deg. <sup>2</sup>	A···Cu distance, Å	PLQY at RT, %	Reference
CsCu <sub>2</sub> Cl <sub>3</sub>	0.26037	363.8477	4.1139	48.0	<sup>10</sup>
Cs <sub>3</sub> Cu <sub>2</sub> Br <sub>5</sub>	0.06466, 0.141130	82.6758, 246.73	3.591(x2), 3.743, 4.012(x2), 4.093, 4.184(x2)	50.1	<sup>11</sup>
K <sub>2</sub> CuBr <sub>3</sub>	0.01217	14.8205	3.637(x2), 3.906, 3.976(x2), 3.987(x2)	55, 87	<sup>12,13</sup>
CsCu <sub>2</sub> Br <sub>3</sub>	0.02890	12.6843	4.29809	18.3	<sup>10</sup>
MACu <sub>2</sub> Br <sub>3</sub>	0.02251	27.1412	4.336, 4.513	0	This article
MACuBr <sub>2</sub>	0.00038	14.6206	4.402(x2), 4.525(x2)	0	This article
FACuBr <sub>2</sub>	0.00613	9.9354	3.8697	0	This article
FA <sub>2</sub> [Cu <sub>4</sub> Br <sub>6</sub> ]	0.00266	2.6449	4.5457, 4.508	0	This article
MA <sub>4</sub> [Cu <sub>2</sub> Br <sub>6</sub> ]	0.01429	13.4794	4.128, 4.205, 4.319, 4.368, 4.459	93	<sup>9</sup>
FA <sub>3</sub> CuBr <sub>4</sub>	0.00778	16.3814	4.985, 4.96, 4.12-4.39-4.76-5.00	0?	This article
Cs <sub>3</sub> Cu <sub>2</sub> I <sub>5</sub>	0.04323, 0.12072	53.2336, 255.4036	3.89, 3.924(x2), 4.146(x2), 4.437, 4.451(x3)	98.7	<sup>11</sup>
CsCu <sub>2</sub> I <sub>3</sub>	0.01782	8.2607	4.5860	3.23	<sup>10</sup>
MACu <sub>2</sub> I <sub>3</sub>	0.01136	17.3062	4.65, 4.79	0	<sup>14</sup>
FACu <sub>2</sub> I <sub>3</sub>	0.01006 0.01319	27.5232 40.4748	4.715*	0	<sup>5</sup>

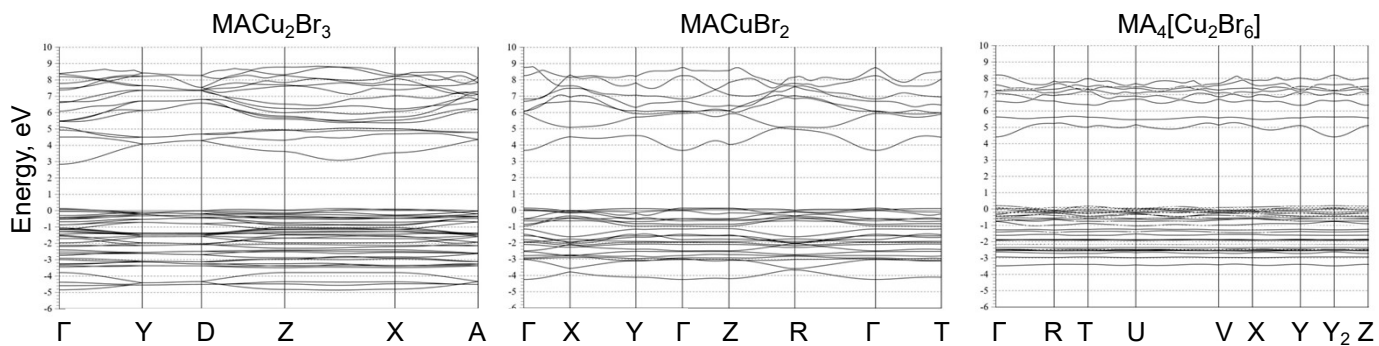


Figure S9. The calculated band structures for  $\text{MACu}_2\text{Br}_3$ ,  $\text{MACuBr}_2$  and  $\text{MA}_4[\text{Cu}_2\text{Br}_6]$  phases.

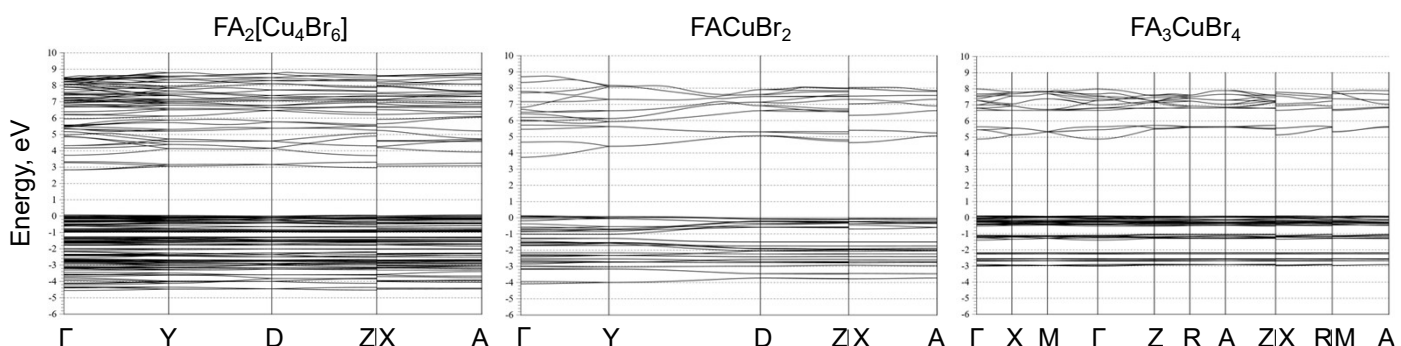


Figure S10. The calculated band structures for  $\text{FA}_2[\text{Cu}_4\text{Br}_6]$ ,  $\text{FACuBr}_2$  and  $\text{FA}_3\text{CuBr}_4$  phases.

## References

- 1 W. H. Baur, *Acta Crystallogr B*, 1974, **30**, 1195–1215.
- 2 K. Robinson, G. v Gibbs and P. H. Ribbe, *Science (1979)*, 1971, **172**, 567–570.
- 3 S. Hull and P. Berastegui, *J Solid State Chem*, 2004, **177**, 3156–3173.
- 4 A. A. Petrov, V. N. Khrustalev, Y. v. Zubavichus, P. v. Dorovatovskii, E. A. Goodilin and A. B. Tarasov, *Mendeleev Communications*, 2018, **28**, 245–247.
- 5 N. Ohashi, Y. Matsushita and N. Saito, *J Solid State Chem*, , DOI:10.1016/j.jssc.2021.122778.
- 6 R. Rocanova, A. Yangui, G. Seo, T. D. Creason, Y. Wu, D. Y. Kim, M. H. Du and B. Saparov, *ACS Mater Lett*, 2019, **1**, 459–465.
- 7 S. Chen, J. Gao, J. Chang, Y. Li, C. Huangfu, H. Meng, Y. Wang, G. Xia and L. Feng, *ACS Appl Mater Interfaces*, 2019, **11**, 17513–17520.
- 8 F. Ge, B. H. Li, P. Cheng, G. Li, Z. Ren, J. Xu and X. H. Bu, *Angewandte Chemie - International Edition*, , DOI:10.1002/anie.202115024.

- 9 H. Peng, S. Yao, Y. Guo, R. Zhi, X. Wang, F. Ge, Y. Tian, J. Wang, B. Zou and B. Zou, *Journal of Physical Chemistry Letters*, 2020, **11**, 4703–4710.
- 10 R. Rocanova, A. Yangui, G. Seo, T. D. Creason, Y. Wu, D. Y. Kim, M.-H. Du and B. Saparov, *ACS Mater Lett*, 2019, **1**, 459–465.
- 11 R. Rocanova, A. Yangui, H. Nhalil, H. Shi, M. H. Du and B. Saparov, *ACS Appl Electron Mater*, 2019, **1**, 269–274.
- 12 T. D. Creason, T. M. McWhorter, Z. Bell, M.-H. H. Du and B. Saparov, *Chemistry of Materials*, 2020, **32**, 6197–6205.
- 13 W. Gao, G. Niu, L. Yin, B. Yang, J.-H. H. Yuan, D. Zhang, K.-H. H. Xue, X. Miao, Q. Hu, X. Du and J. Tang, *ACS Appl Electron Mater*, 2020, **2**, 2242–2249.
- 14 A. V. A. Petrov, S. A. Fateev, A. Yu. Grishko, A. A. Ordinartsev, A. V. A. Petrov, A. Yu. Seregin, P. v. Dorovatovskii, E. A. Goodilin and A. B. Tarasov, *Mendeleev Communications*, 2021, **31**, 14–16.